

Coherent quench dynamics in the one-dimensional Fermi-Hubbard model

Deepak Iyer,¹ Rubem Mondaini,¹ Sebastian Will,² and Marcos Rigol¹

¹*Department of Physics, Pennsylvania State University, University Park, PA 16802, USA*
²*Department of Physics, Massachusetts Institute of Technology, Cambridge, MA 02139, USA*

Recently, it has been shown that the momentum distribution of a metallic state of fermionic atoms in a lattice Fermi-Bose mixture exhibits coherent oscillations after a global quench that suppresses tunneling. The oscillation period is determined by the Fermi-Bose interaction strength. Here we show that similar coherent dynamics, but with a different functional form, occurs in the fermionic Hubbard model when we quench a noninteracting metallic state by introducing a Hubbard interaction and suppressing tunneling. The period is determined primarily by the interaction strength. Conversely, we show that one can accurately determine the Hubbard interaction strength from the oscillation period, taking into account corrections from any small residual tunneling present in the final Hamiltonian. Such residual tunneling shortens the period and damps the oscillations, the latter being visible in the Fermi-Bose experiment.

PACS numbers: 03.75.Ss, 05.30.Fk, 02.30.Ik, 67.85.Lm

a. Introduction. The Hubbard model is one of the simplest models used to describe interacting electrons in solid state materials [1]. It describes spin-1/2 fermions hopping between adjacent sites on a lattice. Opposite-spin fermions interact when they are both present at a site. The model exhibits an interaction-driven metal-insulator transition (Mott transition), and captures physics of strong correlations that is believed to play a fundamental role in high-temperature superconductivity [2–4]. The Mott transition has already been observed at relatively high temperatures with ultracold fermionic atoms loaded in optical lattices [5, 6]. Although achieving lower temperatures remains an experimental challenge, ultracold fermionic systems provide a promising venue to understand the low-temperature phases of the Hubbard model [7].

On a different front, ultracold-atom experiments have begun the exploration of far-from-equilibrium dynamics in isolated many-body quantum systems. Among many remarkable phenomena, it has been possible to observe collapse and revival of matter waves with Bose-Einstein condensates in optical lattices [8, 9], coherent quench dynamics of a Fermi sea in a Fermi-Bose mixture [10], non-thermal behavior in near-integrable experimental regimes [11, 12], and equilibration in Bose-Hubbard-like systems [13]. These experimental findings have motivated a large number of theoretical works seeking to characterize and understand nonequilibrium dynamics in quantum systems [14–16].

We show here that the coherent quench dynamics of the fermionic momentum distribution observed in a lattice Fermi-Bose mixture [10] is a robust phenomenon that also occurs in purely fermionic spin-1/2 systems (see Ref. [17] for other examples of collapse and revival phenomena in bosonic and fermionic systems). In our study, we focus on (noninteracting) metallic initial states at half-filling and their quench dynamics driven by the interacting Hubbard model with suppressed site-to-site tunneling. This is relevant to experiments where the optical lattice is suddenly made very deep. We show that such a

quantum quench leads to long-lived periodic oscillations of each fermionic spin species' momentum distribution. The periodicity of the dynamics depends on the strength of the onsite interaction between the fermions, with quantifiable corrections due to any weak tunneling present in the final Hamiltonian. An experimental measurement of the dynamics can therefore be used to precisely obtain this interaction strength, even in the presence of tunneling.

The coherent quench dynamics observed here relies on off-diagonal (nonlocal) single particle correlations in the initial state and serves as a signature of these. Furthermore, it generally occurs at short times in the transient regime before thermalization takes place. The latter is observed asymptotically after quenches in generic isolated quantum systems [18] and, in particular, in interaction quenches within the Hubbard model in dimensions higher than one [19]. We present our results in the context of the one-dimensional (1D) Hubbard model [4, 20, 21]. Although this model has some fundamental differences from its higher dimensional versions (e.g., it is integrable, which means that it does not thermalize at long times), we do not expect these differences to qualitatively modify our main results [22], which are restricted to the short time dynamics.

Without loss of generality, we focus on the time evolution of the momentum distribution of one of the fermion spin species. First, we present analytical results for the case when the tunneling in the final Hamiltonian is zero, where we find that the momentum distribution oscillates in time with a period governed by the interaction U (this is not expected to change in higher dimensions). Next, we discuss numerical results in the case where a finite, but small, tunneling remains after the quench. We analyze how this modifies the period of the oscillations and leads to damping, and discuss how one can nevertheless accurately extract the interaction strength. Related work in the context of the Bose-Hubbard model was carried out in Ref. [23].

b. Analytical Results. The Hamiltonian for the Hubbard model in a periodic one-dimensional lattice is

$$\hat{H} = \sum_{j=1}^L \left[\sum_{\sigma=\uparrow,\downarrow} \left\{ -t \left(\hat{c}_j^{\sigma\dagger} \hat{c}_{j+1}^\sigma + \text{H.c.} \right) \right\} + U \hat{n}_j^\uparrow \hat{n}_j^\downarrow \right], \quad (1)$$

where $\hat{c}_j^{\sigma\dagger} (\hat{c}_j^\sigma)$ creates (annihilates) a fermion with (pseudo-)spin σ (denoted by \uparrow or \downarrow) at site j , $\hat{n}_j^\sigma = \hat{c}_j^{\sigma\dagger} \hat{c}_j^\sigma$, L is the number of lattice sites, and $\hat{c}_{L+1}^\sigma \equiv \hat{c}_1^\sigma$ sets periodic boundary conditions. We start with an initial metallic state and quench the tunneling to zero. We compute the momentum distribution $n_k^\sigma(\tau) \equiv \langle \hat{c}_k^{\sigma\dagger} \hat{c}_k^\sigma \rangle$ as a function of the time τ after the quench. $\hat{c}_k^{\sigma\dagger} \equiv \sum_{j=1}^L e^{ikaj} \hat{c}_j^{\sigma\dagger} / \sqrt{L}$ creates a fermion with spin- σ and momentum k . Using the results for $n_k^\sigma(\tau)$, we calculate the visibility $\mathcal{V}^\sigma(\tau) = \int_{-k_0}^{k_0} dk n_k^\sigma(\tau)$. It measures the number of fermions with spin σ in the region $[-k_0, k_0]$ of the Brillouin zone. $\mathcal{V}^\sigma(\tau)$ was used in the experiments in Ref. [10] to characterize the time evolution of the momentum distribution after the quench.

The initial Hamiltonian has $t_i = 1$, $U_i = 0$ and the final Hamiltonian has $t_f = 0$, $U_f = U$. For N^\uparrow and N^\downarrow fermions with up and down spins respectively, the initial state (the ground state of the initial Hamiltonian) is a Fermi sea

$$|\psi_0\rangle = \prod_{i=1}^{N^\uparrow} \hat{c}_{k_i^\uparrow}^\dagger \prod_{j=1}^{N^\downarrow} \hat{c}_{k_j^\downarrow}^\dagger |0\rangle. \quad (2)$$

In Eq. (2), $k_j^\sigma = \pm 2\pi j / (aL)$, $j = 0, 1, \dots, (N^\sigma - 1)/2$ for odd N^σ , and a is the lattice spacing. For even N^σ , there is a degeneracy in the ground state due to a partially filled momentum shell. In the analytical calculations, we assume that N^σ is odd (i.e., fully filled momentum shells) and take the thermodynamic limit at the end. The state at time τ after the quench is obtained via the action of the time evolution operator $e^{-i\hat{H}\tau}$, where \hat{H} now contains only the interaction term (we set $\hbar = 1$)

$$|\psi(\tau)\rangle = L^{-\frac{N^\uparrow + N^\downarrow}{2}} \sum_{\{r_j^\sigma\}} \exp \left[-i\tau U \sum_{j=1}^{N^\uparrow} \sum_{l=1}^{N^\downarrow} \delta_{r_j^\uparrow r_l^\downarrow} \right] \times \exp \left[\sum_{j,\sigma} ik_j^\sigma r_j^\sigma \right] \prod_{i=1}^{N^\uparrow} \hat{c}_{r_i^\uparrow}^\dagger \prod_{j=1}^{N^\downarrow} \hat{c}_{r_j^\downarrow}^\dagger |0\rangle. \quad (3)$$

Here, r_j^σ denotes the positions of the fermions in the lattice, $\sum_{\{r_j^\sigma\}}$ implies a sum over all lattice sites for each $j = 1, \dots, N^\sigma$, and $\sigma = \uparrow, \downarrow$. $\delta_{r_j^\uparrow r_l^\downarrow}$ is a Kronecker δ function. As mentioned earlier, the postquench dynamics is due to off-diagonal single particle correlations present in the initial state, which evolve in time. Without loss of generality, we calculate this quantity explicitly for the spin-up fermions, $\langle \hat{c}_m^\dagger \hat{c}_n^\dagger \rangle$. The expectation value is taken in the state at time τ [Eq. (3)]. The

calculation has to be carried out separately for $m = n$ and $m \neq n$. We first obtain the fermion overlaps $\langle 0 | \left[\prod_{\sigma=\uparrow,\downarrow} \prod_{j=1}^{N^\sigma} \hat{c}_{r_j^\sigma}^\sigma \right] \hat{c}_m^\dagger \hat{c}_n^\dagger \left[\prod_{\sigma=\uparrow,\downarrow} \prod_{j=1}^{N^\sigma} \hat{c}_{r_j^\sigma}^{\sigma\dagger} \right] |0\rangle$ as determinants of δ functions (see Supplementary Material). After summing over the δ functions and simplifying the time-dependent exponents, we obtain for $m \neq n$

$$\langle \psi(\tau) | c_m^\dagger c_n^\dagger | \psi(\tau) \rangle = L^{-N^\downarrow - 1} \left[\sum_{l=1}^{N^\uparrow} e^{ik_l^\uparrow (n-m)} \right] \times \sum_Q \text{sgn}(Q) \prod_{j=1}^{N^\downarrow} \left[\delta_{Q_j j} + (e^{-i\tau U} - 1) e^{i(k_j^\downarrow - k_{Q_j}^\downarrow)n} + (e^{i\tau U} - 1) e^{i(k_j^\downarrow - k_{Q_j}^\downarrow)m} \right], \quad (4)$$

where Q are permutations over $\{1, \dots, N^\downarrow\}$. The sum over permutations of the product in the brackets is essentially a determinant. It can be evaluated explicitly using the matrix determinant lemma (see Supplementary Material). For $m = n$, $\langle \hat{c}_m^\dagger \hat{c}_m^\dagger \rangle$ is the mean site occupation, which is constant in time. Its value is $n^\uparrow \equiv N^\uparrow / L$. We finally convert the sums over momenta to integrals by taking the thermodynamic limit to get

$$\langle \psi(\tau) | c_m^\dagger c_n^\dagger | \psi(\tau) \rangle = (1 - \delta_{mn}) \frac{\sin[\pi n^\uparrow (m-n)]}{\pi(m-n)} \times \left[1 + 2n^\downarrow (n^\downarrow - 1) (1 - \cos U\tau) - 2(1 - \cos U\tau) \frac{\sin^2[\pi n^\downarrow (m-n)]}{\pi^2 (m-n)^2} \right] + n^\uparrow \delta_{mn}. \quad (5)$$

It can be verified that at $\tau = 0$ we recover the single-particle correlations of free fermions for $m \neq n$ and the site occupancies for $m = n$. Equation (5) already hints at the occurrence of coherent oscillations of the momentum distribution in time. Notice the presence of terms proportional to $\cos U\tau$. For comparison, in the Fermi-Bose case, one obtains an exponential of a cosine of $U\tau$ [10]. This means that while on dimensional grounds the time scale for oscillations must be proportional to $1/U$, the functional form of the time dependence is nontrivial and depends on the system being considered.

By Fourier transforming Eq. (5), we obtain the momentum distribution function. The time evolution of the occupation of the $k = 0$ mode for $n^\uparrow = n^\downarrow = 1/2$, i.e., at half-filling, has the following particularly simple form:

$$n_{k=0}^{\text{half-filling}}(\tau) = 1 - \frac{3}{8}(1 - \cos U\tau). \quad (6)$$

By integrating the momentum distribution in the region $[-k_0, k_0]$, we obtain the visibility

$$\mathcal{V}(\tau) = \frac{k_0}{\pi\nu} + 2g(k_0, \nu)(1 - \cos U\tau), \quad (7)$$

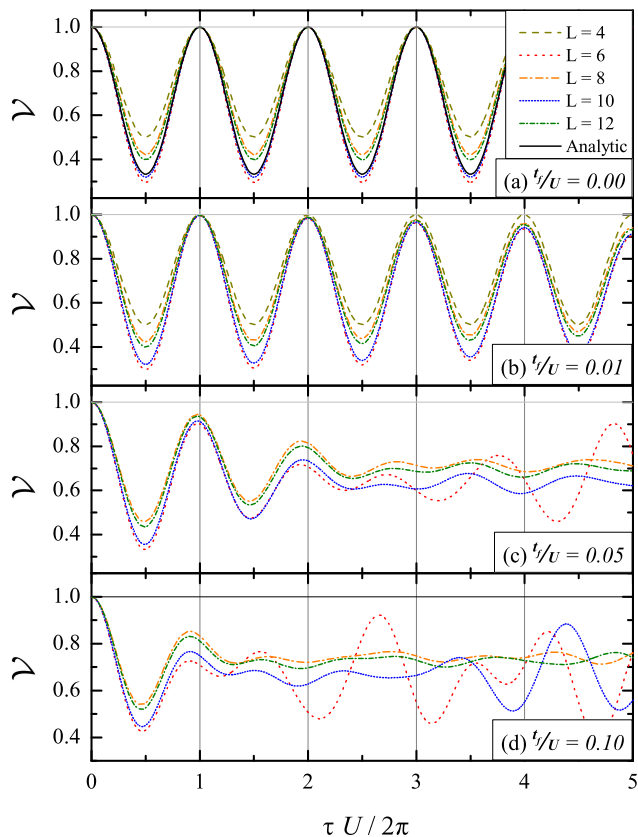


FIG. 1. (Color online) Visibility as a function of time for a half-filled metallic initial state and different values of the final hopping amplitude t_f [(a)–(d)]. We take k_0 to be the Fermi momentum in the initial state. The curves in each panel correspond to different system sizes L (4, 6, 8, 10 and 12). Panels (a)–(d) show that there is a decrease in the revival time and an increase in damping, as the hopping amplitude t_f increases. The solid (black) curve in panel (a) depicts the analytical result for $t_f = 0$ in the thermodynamic limit [Eq. (7)]. Panel (a) shows that the systems with $L = 4, 8,$ and 12 exhibit the largest finite-size effects. Also, note that with increasing system size they approach the thermodynamic limit result from above, while those with $L = 6$ and 10 approach the thermodynamic limit result from below. The case $L = 4$ is not displayed in panels (c) and (d) for clarity. Note that panels (c) and (d) show additional revivals for some system sizes. These are due to finite-size effects. All quantities plotted are dimensionless

where $g(k_0, \nu)$ is composed of polylog functions (see Supplementary Material for details), $\nu \equiv n^{\uparrow, \downarrow} = N^{\uparrow, \downarrow}/L$ is the filling fraction (we assume $N^{\uparrow} = N^{\downarrow}$ such that $\mathcal{V}^{\uparrow} = \mathcal{V}^{\downarrow} \equiv \mathcal{V}$), and $k_0 \leq \pi\nu$. As a check, $g(k_0, 1) = 0$ as expected, because for a fully filled Brillouin zone no dynamics is possible.

c. Exact Diagonalization Results. In what follows, we use full exact diagonalization to understand how the analytical results in the absence of tunneling in the final Hamiltonian are modified in the presence of a finite, but small, tunneling amplitude. We study lattices of length $L = 4, 6, 8, 10,$ and 12 at half-filling. For lattice sizes

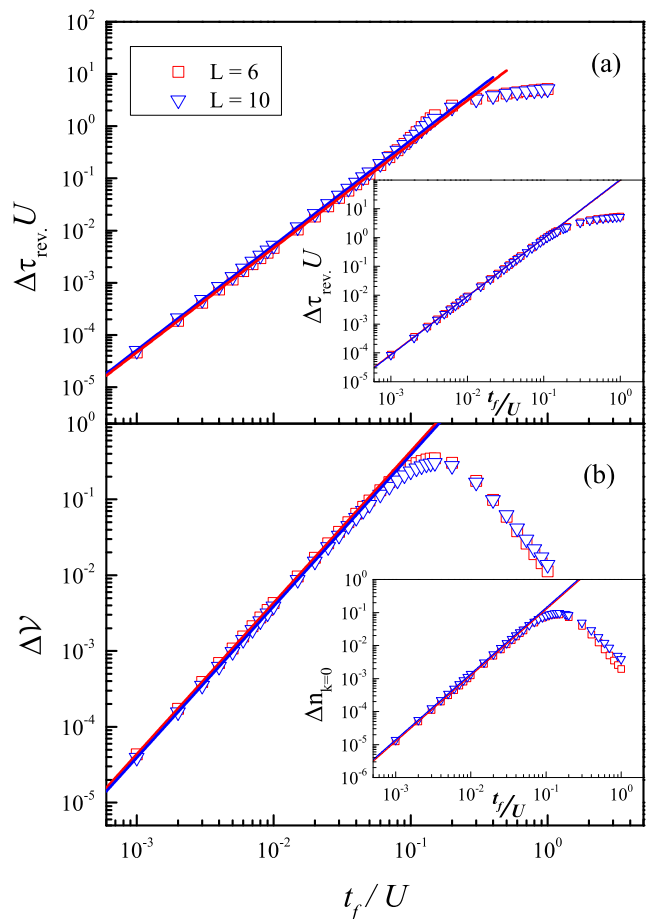


FIG. 2. (Color online) (a) Absolute value of the shift in the visibility revival time as a function of the final hopping t_f . (b) Damping (defined as the absolute value of the change of \mathcal{V} at the first revival, from the $t_f = 0$ result) as a function of t_f . The insets show the corresponding results for the zero-momentum occupation of one of the species ($n_{k=0}$). All panels display results for systems with $L = 6$ and 10 , as they exhibit the smallest finite-size effects. All quantities plotted are dimensionless.

$L = 4m$ ($m = 1, 2, \dots$), the initial ground state is four-fold degenerate due to partially filled momentum shells in the noninteracting Fermi sea. We use translation and parity symmetries and focus on the even parity sector within the total quasimomentum $k = 0$ sector, where the ground state is not degenerate. The resulting reduction in the size of the relevant Hilbert space allows us to study the exact many-body dynamics in sufficiently large systems for arbitrarily long times.

In Fig. 1, we show exact diagonalization results for the visibility as a function of time for different values of t_f and for the five system sizes studied. Figure 1(a) depicts results for $t_f = 0$, where we also include the analytical results in the thermodynamic limit [Eq. (7)]. A comparison between the exact diagonalization results and the analytic ones makes apparent that the systems with $L = 4m$ ($L = 4, 8,$ and 12 , for $m = 1, 2$ and 3 , respectively),

which correspond to partially filled momentum shells in the noninteracting Fermi sea, suffer from stronger finite-size effects than those with $L = 4m + 2$ ($L = 6$ and 10 , for $m = 1$ and 2 , respectively), which correspond to completely filled momentum shells in the noninteracting Fermi sea. However, with increasing system size, they all seem to approach the analytic prediction in the thermodynamic limit.

As one moves away from the ideal $t_f = 0$ case and increases t_f , two effects are clearly visible in our results for the visibility in Fig. 1: the time it takes for the system to have the first revival decreases, and the maximum value of the visibility at the first revival decreases, i.e., damping increases. This is because in the presence of finite tunneling the local occupations are not good quantum numbers. Their change with time leads to decoherence in the many-body dynamics and, consequently, to damping of the oscillations. A finite small tunneling can be thought of as a perturbation to the $t_f = 0$ case. Hence, all nonconserved quantities and parameters will exhibit perturbative corrections proportional to powers of t_f/U . For the largest tunneling amplitudes shown, $t_f/U = 0.05$ [Fig. 2(c)] and $t_f/U = 0.1$ [Fig. 2(d)], finite-size effects lead to large revivals of the visibility after a few oscillation periods. They also lead to sizable differences between the values of \mathcal{V} even at the first revival, while the time of the first revival is barely affected by finite-size effects. As t_f/U increases, deviations from periodic dynamics become apparent after the first oscillation periods [see, e.g., Fig. 2(d)].

In Fig. 2, we study the change in the revival time (by which we mean the time of the first revival) and damping as a function of the final tunneling t_f , starting with very small values of t_f . We find that the deviation in the revival time from the value at $t_f = 0$ scales as t_f^2 if U is unchanged [Fig. 2(a)]. This is straightforward to understand. The revival time τ_{rev} has a functional form $\tau_{\text{rev}}(t_f, U) = 2\pi T(t_f/U)/U$, T being some dimensionless function of t_f/U . For small t_f/U , a perturbative expansion of T has a quadratic subleading term (the leading term being 1) — a linear term is not allowed since the Hubbard model in a bipartite lattice is invariant under a change $t \rightarrow -t$. By a fit to the numerical data for $L = 10$, we find that $\Delta\tau_{\text{rev}} \equiv \tau_{\text{rev}}(0, U) - \tau_{\text{rev}}(t_f, U) = 2\pi C t_f^2/U^3$, with $C = 8.7 \pm 0.1$. Similarly, we find that $\Delta\mathcal{V} \equiv \mathcal{V}_{\text{max}}(0, U) - \mathcal{V}_{\text{max}}(t_f, U) = D t_f^2/U^2$ with $D = 38.46 \pm 0.04$. By $\mathcal{V}_{\text{max}}(0, U)$ and $\mathcal{V}_{\text{max}}(t_f, U)$, we mean the maximum of the visibility in the first revival for $t_f = 0$ and $t_f \neq 0$, respectively. In Fig. 2, finite-size effects can be seen to be slightly larger for $\Delta\mathcal{V}$ than for $\Delta\tau_{\text{rev}}$ so the results obtained for the latter are expected

to be closer to the thermodynamic limit result.

If one studies the dynamics of the occupation of the $k = 0$ mode of one of the spin species ($n_{k=0}$), the results obtained are qualitatively similar to those for the visibility [see the insets in Fig. 2 and Eq. (6)], which means that such an observable can also be used in the experiments to study collapse and revival phenomena in fermionic systems.

Remarkably, one can accurately determine the on-site interaction strength U in an experiment that has a small finite value of t_f by using the measured revival time. First, the value of t_f can be calculated from the known experimental lattice parameters [24]. Since the revival time is given by $\tau_{\text{rev}} = (2\pi/U)[1 - C t_f^2/U^2]$, the experimentally measured value of τ_{rev} , in combination with the calculated value of t_f and the result obtained here for C (or more precise ones which could be obtained, e.g., using time-dependent density matrix renormalization group [25]) allows one to obtain U by solving the cubic equation $\tau_{\text{rev}} U^3/2\pi - U^2 + C t_f^2 = 0$. This can also be done for bosonic systems [23].

d. Summary. We have shown that the momentum distribution function of a spin-1/2 metallic system exhibits coherent oscillations after a quench to a finite interaction strength and suppressed tunneling. Similar to the Fermi-Bose case [10], nontrivial off-diagonal single-particle correlations in the initial state and on-site interactions in the final Hamiltonian are responsible for the dynamics. Experimental observation of such dynamics would therefore provide evidence for those off-diagonal correlations. We have obtained analytical results for $t_f = 0$ in the thermodynamic limit, and compared them to those obtained using full exact diagonalization of finite systems. This allowed us to gauge finite-size effects in the exact diagonalization calculations. The results for $L = 10$ were found to be closest to those in the thermodynamic limit. Using exact diagonalization, we showed that small finite residual tunneling after the quench causes damping of the oscillations and modifies the revival time. We argued that using the measured period of the first oscillation from experimental data, and our (or others) theoretical results for the constant C , one can obtain the interaction strength very accurately.

ACKNOWLEDGMENTS

This work was supported by the U.S. Office of Naval Research (D.I. and M.R.), by the National Science Foundation Grant No. PHY13-18303 (R.M. and M.R.) and by CNPq (R.M.).

[1] J. Hubbard, Proc. R. Soc. London A **276**, 238 (1963).
 [2] E. Dagotto, Rev. Mod. Phys. **66**, 763 (1994).

[3] M. Imada, A. Fujimori, and Y. Tokura, Rev. Mod. Phys. **70**, 1039 (1998).
 [4] E. H. Lieb and F. Wu, Physica A **321**, 1 (2003).

- [5] R. Jördens, N. Strohmaier, K. Günter, H. Moritz, and T. Esslinger, *Nature (London)* **455**, 204 (2008).
- [6] U. Schneider, L. Hackermüller, S. Will, T. Best, I. Bloch, T. A. Costi, R. W. Helmes, D. Rasch, and A. Rosch, *Science* **322**, 1520 (2008).
- [7] T. Esslinger, *Annual Review of Condensed Matter Physics* **1**, 129 (2010).
- [8] M. Greiner, O. Mandel, T. W. Hänsch, and I. Bloch, *Nature* **419**, 51 (2002).
- [9] S. Will, T. Best, S. Braun, U. Schneider, and I. Bloch, *Phys. Rev. Lett.* **106**, 115305 (2011).
- [10] S. Will, D. Iyer, and M. Rigol, ArXiv:1406.2669.
- [11] T. Kinoshita, T. Wenger, and D. S. Weiss, *Nature* **440**, 900 (2006).
- [12] M. Gring, M. Kuhnert, T. Langen, T. Kitagawa, B. Rauer, M. Schreitl, I. Mazets, D. A. Smith, E. Demler, and J. Schmiedmayer, *Science* **337**, 1318 (2012).
- [13] S. Trotzky, Y.-A. Chen, A. Flesch, I. P. McCulloch, U. Schollwöck, J. Eisert, and I. Bloch, *Nature Phys.* **8**, 325 (2012).
- [14] M. A. Cazalilla and M. Rigol, *New J. Phys.* **12**, 055006 (2010).
- [15] J. Dziarmaga, *Adv. Phys.* **59**, 1063 (2010).
- [16] A. Polkovnikov, K. Sengupta, A. Silva, and M. Vengalattore, *Rev. Mod. Phys.* **83**, 863 (2011).
- [17] K. Mahmud, L. Jiang, P. Johnson, and E. Tiesinga, arXiv:1401.6648 (2014).
- [18] M. Rigol, V. Dunjko, and M. Olshanii, *Nature* **452**, 854 (2008).
- [19] M. Eckstein, M. Kollar, and P. Werner, *Phys. Rev. Lett.* **103**, 056403 (2009).
- [20] E. H. Lieb and F. Y. Wu, *Phys. Rev. Lett.* **20**, 1445 (1968).
- [21] F. Essler, H. Frahm, F. Göhmann, A. Klümper, and V. Korepin, *The One-Dimensional Hubbard Model* (Cambridge University Press, 2005).
- [22] At least for bipartite lattices.
- [23] F. A. Wolf, I. Hen, and M. Rigol, *Phys. Rev. A* **82**, 043601 (2010).
- [24] W. Zwerger, *J. Opt. B* **5**, S9 (2003).
- [25] U. Schollwöck, *Rev. Mod. Phys.* **77**, 259 (2005).
- [26] A. G. Akritas, E. K. Akritas, and G. I. Malaschonok, *Mathematics and Computers in Simulation* **42**, 585 (1996).

SUPPLEMENTARY MATERIAL

We show details of the calculations leading to Eq. (7). From the state at finite-time τ after the quench, we calculate the single-particle density matrix $\langle c_m^\dagger c_n^\dagger \rangle$. For $m \neq n$, we have

$$\begin{aligned}
\langle \psi(\tau) | c_m^\dagger c_n^\dagger | \psi(\tau) \rangle &= \sum_{\{r_j^{\uparrow,\downarrow}\}} \sum_{\{r_j^{\prime\uparrow,\downarrow}\}} e^{\sum_j i k_j^\dagger (r_j^\dagger - r_j^{\prime\uparrow}) + i k_j^\downarrow (r_j^\downarrow - r_j^{\prime\downarrow})} e^{-i\tau U \sum_{i,j} (\delta_{r_i^\dagger r_j^\dagger} - \delta_{r_i^{\prime\uparrow} r_j^{\prime\downarrow})} \langle 0 | \prod_{j=1}^N c_{r_j^\dagger}^\dagger c_{r_j^\downarrow}^\downarrow c_m^\dagger c_n^\dagger \prod_{j=1}^N c_{r_j^\dagger}^\dagger c_{r_j^\downarrow}^\downarrow | 0 \rangle \\
&= \sum_{\{r_j^{\prime\uparrow,\downarrow}\}} \sum_{\{r_j^{\uparrow,\downarrow}\}} e^{\sum_j i k_j^\dagger (r_j^\dagger - r_j^{\prime\uparrow}) + i k_j^\downarrow (r_j^\downarrow - r_j^{\prime\downarrow})} e^{-i\tau U \sum_{i,j} (\delta_{r_i^\dagger r_j^\dagger} - \delta_{r_i^{\prime\uparrow} r_j^{\prime\downarrow})} \left[\sum_P \sigma^P \prod_{j=1}^N \delta_{r_j^\dagger, r_j^{\prime\downarrow}} \right] \left[\sum_Q \sigma^Q \delta_{nr_i^\dagger} \delta_{mr_i^{\prime\downarrow}} \prod_{i \neq l} \delta_{r_{Q_i}^\dagger r_i^\dagger} \right] \\
&= \sum_{\{r_j^{\prime\uparrow}, r_j^{\prime\downarrow}\}} \sum_{\{r_j^\dagger, r_j^\downarrow\}} \sum_{P,Q} \sum_l \sigma^P \sigma^Q e^{\sum_j i (k_j^\dagger r_j^\dagger - k_{Q_j}^\dagger r_j^{\prime\uparrow}) + i (k_j^\downarrow - k_{P_j}^\downarrow) r_j^\downarrow} e^{-i\tau U \sum_{i,j} (\delta_{r_i^\dagger r_j^\dagger} - \delta_{r_i^{\prime\uparrow} r_{P_j}^\downarrow})} \left[\delta_{nr_i^\dagger} \delta_{mr_i^{\prime\downarrow}} \prod_{i \neq l} \delta_{r_{Q_i}^\dagger r_i^\dagger} \right] \\
&= \sum_l \sum_{\{r_j^\dagger, j \neq l\}} \sum_{\{r_j^\downarrow\}} \sum_{P,Q} \sigma^P \sigma^Q \left[e^{\sum_{j \neq l} i (k_j^\dagger - k_{Q_j}^\dagger) r_j^\dagger + i (k_j^\downarrow - k_{P_j}^\downarrow) r_j^\downarrow} e^{-i\tau U \sum_{i \neq l, j} (\delta_{r_i^\dagger r_j^\dagger} - \delta_{r_i^{\prime\uparrow} r_{P_j}^\downarrow})} \right] \\
&\quad \times e^{i (k_l^\dagger n - k_{Q_l}^\dagger m) + i (k_l^\downarrow - k_{P_l}^\downarrow) r_l^\downarrow} e^{-i\tau U \sum_j (\delta_{nr_j^\dagger} - \delta_{mr_j^\downarrow})}
\end{aligned} \tag{8}$$

Due to the double sum in the time-dependent exponent, a dramatic simplification occurs:

$$\begin{aligned}
\langle \psi(\tau) | c_m^\dagger c_n^\dagger | \psi(\tau) \rangle &= \sum_Q \sigma^Q \sum_l \sum_{\{r_j^\dagger, j \neq l\}} \sum_{\{r_j^\downarrow\}} \sum_P \sigma^P \left[\prod_{j \neq l} e^{i(k_j^\dagger - k_{P_j}^\dagger)r_j^\dagger + i(k_j^\downarrow - k_{P_j}^\downarrow)r_j^\downarrow} \right] \\
&\quad \times e^{i(k_l^\dagger n - k_{P_l}^\dagger m) + i(k_l^\downarrow - k_{P_l}^\downarrow)r_l^\downarrow} e^{-i\tau U \sum_j (\delta_{nr_j^\downarrow} - \delta_{mr_j^\downarrow})} \\
&= \sum_Q \sigma^Q L^{N^\dagger - 1} \sum_{l=1}^{N^\dagger} e^{ik_l^\dagger(n-m)} \prod_{j=1}^{N^\downarrow} \sum_{r_j^\downarrow} e^{i(k_j^\downarrow - k_{Q_j}^\downarrow)r_j^\downarrow} e^{-i\tau U (\delta_{nr_j^\downarrow} - \delta_{mr_j^\downarrow})} \\
&= \sum_Q \sigma^Q L^{N^\dagger - 1} \sum_{l=1}^{N^\dagger} e^{ik_l^\dagger(n-m)} \prod_{j=1}^{N^\downarrow} \sum_{r_j^\downarrow} e^{i(k_j^\downarrow - k_{Q_j}^\downarrow)r_j^\downarrow} [1 + (e^{-i\tau U} - 1)\delta_{nr_j^\downarrow} + (e^{i\tau U} - 1)\delta_{mr_j^\downarrow}] \\
&= L^{N^\dagger - 1} \left[\sum_{l=1}^{N^\dagger} e^{ik_l^\dagger(n-m)} \right] \sum_Q \sigma^Q \prod_{j=1}^{N^\downarrow} \left[\frac{\sin[(k_j^\downarrow - k_{Q_j}^\downarrow)L/2]}{\sin[(k_j^\downarrow - k_{Q_j}^\downarrow)/2]} + (e^{-i\tau U} - 1)e^{i(k_j^\downarrow - k_{Q_j}^\downarrow)n} + (e^{i\tau U} - 1)e^{i(k_j^\downarrow - k_{Q_j}^\downarrow)m} \right] \\
&= L^{N^\dagger - 1} \left[\sum_{l=1}^{N^\dagger} e^{ik_l^\dagger(n-m)} \right] L^{N^\downarrow} \left[1 + 2 \left\{ \frac{N^\downarrow(N^\downarrow - 1)}{L^2} - \frac{N^\downarrow}{L} \right\} (1 - \cos U\tau) - 2(1 - \cos U\tau)L^{-2} \sum_{i,j=1}^{N^\downarrow} e^{i(m-n)(k_i^\downarrow - k_j^\downarrow)} \right] \\
&= L^{N^\dagger + N^\downarrow - 1} \left[\sum_{l=1}^{N^\dagger} e^{ik_l^\dagger(n-m)} \right] \left[1 + 2n^\downarrow(n^\downarrow - 1)(1 - \cos U\tau) - 2(1 - \cos U\tau)L^{-2} \sum_{i,j=1}^{N^\downarrow} e^{i(m-n)(k_i^\downarrow - k_j^\downarrow)} \right]
\end{aligned} \tag{9}$$

In the second to last line, we have evaluated the sum over permutations Q – it is essentially the determinant of a matrix \mathbf{A} whose elements are

$$A_{ij} = L\delta_{ij} + \alpha e^{i(k_i^\downarrow - k_j^\downarrow)n} + \alpha^* e^{i(k_i^\downarrow - k_j^\downarrow)m} \tag{10}$$

where we have taken into account that in the limit of large L the first term vanishes unless $k_i^\downarrow = k_j^\downarrow$, and set $\alpha = e^{-iU\tau} - 1$. Introducing the following vectors

$$\begin{aligned}
[\mathbf{u}]_j &= \alpha e^{ik_j^\downarrow n}, & [\mathbf{v}]_j &= e^{-ik_j^\downarrow n}, \\
[\mathbf{u}']_j &= \alpha^* e^{ik_j^\downarrow m}, & [\mathbf{v}']_j &= e^{-ik_j^\downarrow m},
\end{aligned} \tag{11}$$

the matrix \mathbf{A} can be written as

$$\begin{aligned}
\mathbf{A} &= L\mathbf{1} + \mathbf{u}\mathbf{v}^T + \mathbf{u}'\mathbf{v}'^T \\
&= L\mathbf{1} + (\mathbf{u} \ \mathbf{u}') \begin{pmatrix} \mathbf{v}^T \\ \mathbf{v}'^T \end{pmatrix}
\end{aligned} \tag{12}$$

We then use the Matrix Determinant lemma (or Sylvester's theorem) [26] to write the determinant of \mathbf{A} as

$$\begin{aligned}
\det \mathbf{A} &= L^{N^\downarrow} \det \left[\mathbf{1} + L^{-1} \begin{pmatrix} \mathbf{v}^T \\ \mathbf{v}'^T \end{pmatrix} (\mathbf{u} \ \mathbf{u}') \right] \\
&= L^{N^\downarrow} [(1 + L^{-1}\mathbf{v}^T \mathbf{u})(1 + L^{-1}\mathbf{v}'^T \mathbf{u}') - L^{-2}\mathbf{v}^T \mathbf{u}' \mathbf{v}'^T \mathbf{u}] \\
&= L^{N^\downarrow} \left[(1 + \alpha n^\downarrow)(1 + \alpha^* n^\downarrow) - L^{-2}\alpha\alpha^* \sum_{i,j} e^{i(k_i^\downarrow - k_j^\downarrow)(m-n)} \right] \\
&= L^{N^\downarrow} \left[1 + 2(1 - \cos U\tau)n^\downarrow(n^\downarrow - 1) - 2L^{-2}(1 - \cos U\tau) \sum_{i,j} e^{i(k_i^\downarrow - k_j^\downarrow)(m-n)} \right].
\end{aligned} \tag{13}$$

For $m = n$, the above calculation can be repeated, and results in

$$\begin{aligned} \langle \psi(\tau) | c_m^\dagger c_n^\dagger | \psi(\tau) \rangle &= L^{N^\uparrow - 1} \sum_{l=1}^{N^\uparrow} \prod_{j=1}^{N^\downarrow} \sum_{r_j^\downarrow} \delta_{mn} e^{i(k_j^\downarrow - k_{Q_j}^\downarrow) r_j^\downarrow} \\ &= N^\uparrow L^{N^\uparrow + N^\downarrow - 1} \delta_{mn}. \end{aligned} \quad (14)$$

Normalizing both expressions, we finally get

$$\begin{aligned} \langle \psi(\tau) | c_m^\dagger c_n^\dagger | \psi(\tau) \rangle &= \\ (1 - \delta_{mn}) L^{-1} \left[\sum_{l=1}^{N^\uparrow} e^{i k_l^\uparrow (n-m)} \right] &\left[1 + 2n^\downarrow (n^\downarrow - 1) (1 - \cos U\tau) - 2L^{-2} (1 - \cos U\tau) \sum_{i,j=1}^{N^\downarrow} e^{i(m-n)(k_i^\downarrow - k_j^\downarrow)} \right] + n^\uparrow \delta_{mn}. \end{aligned} \quad (15)$$

The momentum distribution is given by

$$n_k^\uparrow = L^{-1} \sum_{m,n} e^{i k (m-n)} \langle c_m^\dagger c_n^\dagger \rangle. \quad (16)$$

The sums over the momenta can be converted to integrals in the thermodynamic limit. However, it is important that we do not change the sum over m, n to an integral (the lattice is fundamental)

$$\begin{aligned} n_k(\tau) &= \sum_{m,n} e^{i k (m-n)} \left\{ L^{-1} \left[\int_{-k_F}^{k_F} \frac{dk^\uparrow}{2\pi} e^{i k^\uparrow (n-m)} \right] \left[1 + 2n^\downarrow (n^\downarrow - 1) (1 - \cos U\tau) - 2(1 - \cos U\tau) \right. \right. \\ &\quad \left. \left. \times \int_{-k_F}^{k_F} \frac{dk_1^\downarrow}{2\pi} \frac{dk_2^\downarrow}{2\pi} e^{i(m-n)(k_1^\downarrow - k_2^\downarrow)} \right] \right. \\ &\quad \left. + L^{-1} \delta_{mn} (n^\uparrow - n^\uparrow [1 + 2n^\downarrow (n^\downarrow - 1) (1 - \cos U\tau) - 2(1 - \cos U\tau) (n^\downarrow)^2]) \right\} \\ &= \sum_{m,n} e^{i k (m-n)} \left\{ L^{-1} \frac{\sin(\pi n^\uparrow (m-n))}{\pi(m-n)} \left[1 + 2n^\downarrow (n^\downarrow - 1) (1 - \cos U\tau) - 2(1 - \cos U\tau) \frac{\sin^2(\pi n^\downarrow (m-n))}{\pi^2 (m-n)^2} \right] \right. \\ &\quad \left. + L^{-1} \delta_{mn} 2n^\downarrow n^\uparrow (1 - \cos U\tau) \right\} \\ &= \sum_{m,n} e^{i k (m-n)} \left\{ L^{-1} \frac{\sin(\pi n^\uparrow (m-n))}{\pi(m-n)} \left[1 + 2n^\downarrow (n^\downarrow - 1) (1 - \cos U\tau) - 2(1 - \cos U\tau) \frac{\sin^2(\pi n^\downarrow (m-n))}{\pi^2 (m-n)^2} \right] \right. \\ &\quad \left. + L^{-1} \delta_{mn} 2n^\downarrow n^\uparrow (1 - \cos U\tau) \right\}. \end{aligned} \quad (17)$$

The occupation of the $k = 0$ momentum mode is given by

$$\begin{aligned} n_{k=0}(\tau) &= \sum_{m,n} \left\{ L^{-1} \frac{\sin(\pi n^\uparrow (m-n))}{\pi(m-n)} \left[1 + 2n^\downarrow (n^\downarrow - 1) (1 - \cos U\tau) - 2(1 - \cos U\tau) \frac{\sin^2(\pi n^\downarrow (m-n))}{\pi^2 (m-n)^2} \right] \right. \\ &\quad \left. + L^{-1} \delta_{mn} 2n^\downarrow n^\uparrow (1 - \cos U\tau) \right\} \\ &= \sum_{m^-} \left\{ \frac{\sin(\pi n^\uparrow m^-)}{\pi m^-} \left[1 + 2n^\downarrow (n^\downarrow - 1) (1 - \cos U\tau) - 2(1 - \cos U\tau) \frac{\sin^2(\pi n^\downarrow m^-)}{\pi^2 (m^-)^2} \right] \right\} + 2n^\downarrow n^\uparrow (1 - \cos U\tau) \\ &= [1 + 2n^\downarrow (n^\downarrow - 1) (1 - \cos U\tau) - 2(1 - \cos U\tau) f(n^\uparrow, n^\downarrow)] + 2n^\downarrow n^\uparrow (1 - \cos U\tau) \\ &= 1 + 2(1 - \cos U\tau) [n^\downarrow (n^\uparrow + n^\downarrow - 1) - f(n^\uparrow, n^\downarrow)], \end{aligned} \quad (18)$$

where

$$f(n^\uparrow, n^\downarrow) = (n^\downarrow)^2 n^\uparrow + \frac{i}{4\pi^3} \left[2 \text{Li}_3(e^{-i\pi n^\uparrow}) + \text{Li}_3(e^{i\pi(2n^\downarrow + n^\uparrow)}) + \text{Li}_3(e^{-i\pi(2n^\downarrow - n^\uparrow)}) - \text{c.c.} \right], \quad (19)$$

and $\text{Li}_s(z) \equiv \sum_{k=1}^{\infty} \frac{z^k}{k^s}$ is the polylogarithm function. For $n^\uparrow = n^\downarrow = 1/2$, we get

$$n_{k=0}^{\text{half-filling}}(\tau) = 1 - \frac{3}{8}(1 - \cos U\tau) \quad (20)$$

To compute the visibility, for simplicity, we assume that $\nu \equiv n^\uparrow = n^\downarrow = k_F/\pi$ and that $k_0 < k_F$. We get that, for $k_0 \leq \pi\nu$,

$$\begin{aligned} \mathcal{V}(\tau) &= \frac{1}{n^\uparrow} \sum_{m,n} \frac{\sin(k_0(m-n))}{\pi(m-n)} \left\{ L^{-1} \frac{\sin(\pi n^\uparrow(m-n))}{\pi(m-n)} \left[1 + 2n^\downarrow(n^\downarrow - 1)(1 - \cos U\tau) - 2(1 - \cos U\tau) \frac{\sin^2(\pi n^\downarrow(m-n))}{\pi^2(m-n)^2} \right] \right. \\ &\quad \left. + L^{-1} \delta_{mn} 2n^\downarrow n^\uparrow (1 - \cos U\tau) \right\} \\ &= \frac{k_0}{\pi\nu} [1 + 2\nu(\nu - 1)(1 - \cos U\tau)] + 2(1 - \cos U\tau)g(k_0, \nu) + 2\frac{k_0}{\pi}\nu^2(1 - \cos U\tau) \\ &= \frac{k_0}{\pi\nu} + 2g(k_0, \nu)(1 - \cos U\tau), \end{aligned} \quad (21)$$

where $g(k_0, \nu)$ is given by:

$$\begin{aligned} g(k_0, \nu) &= \frac{k_0\nu}{\pi} + \frac{k_0(\nu - 1)}{\pi} - \frac{k_0\nu^2}{\pi} + \frac{1}{8\pi^4\nu} \left[\text{Li}_4(e^{-i(k_0 - 3\pi\nu)}) + \text{Li}_4(e^{i(k_0 - 3\pi\nu)}) - \text{Li}_4(e^{-i(k_0 + 3\pi\nu)}) - \text{Li}_4(e^{i(k_0 + 3\pi\nu)}) \right. \\ &\quad \left. + 3\text{Li}_4(e^{-i(k_0 + 3\pi\nu)}) + 3\text{Li}_4(e^{i(k_0 + 3\pi\nu)}) - 3\text{Li}_4(e^{-i(k_0 - 3\pi\nu)}) - 3\text{Li}_4(e^{i(k_0 - 3\pi\nu)}) \right]. \end{aligned} \quad (22)$$